Supplementary Information: Osmolyte-induced Conformational Stabilization of a Hydrophobic Polymer

Pooja Nanavare,[1] Soham Sarkar,[2] Abhijit Bijay Jena,[1] and Rajarshi Chakrabarti[1, *]

[1] *Department of Chemistry, Indian Institute of Technology Bombay, Mumbai 400076, India*
[2] *Eduard-Zintl-Institute für Anorganische und Physikalische Chemie,*
Technische Universität Darmstadt, Alarich-Weiss-Strasse8, 64287 Darmstadt, Germany
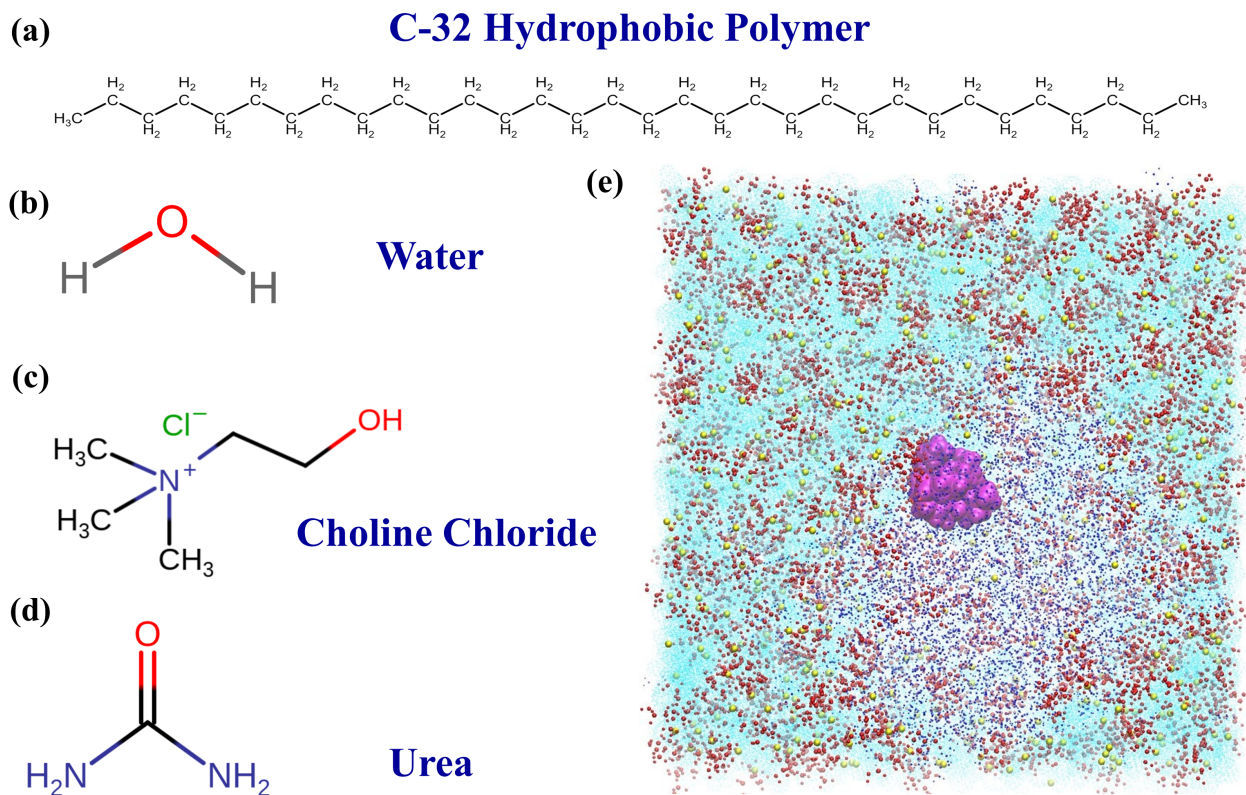
SYSTEM DETAILS

Fig. S1. Chemical structure of (a) C-32 hydrophobic polymer, (b) water, (c) choline chloride, (d) urea, and (e) a representative configuration of system containing hydrophobic polymer in collapsed conformation (magenta color) in water (cyan color), urea (blue color), choline (red color), and chloride (yellow color). Polymer is represented in VDW representation and urea, choline chloride are shown in beads and water in surface representations for visuallization purpose.

Sr. No.	System	No. of Water	No. of Choline	No. of Chloride	No. of Urea	Box Edge Length (nm)	Unbiased Simulations (ns)	Biased Simulations (ns)	Simulations with frozen state (ns)
1	PW	6875	-	-	-	5.91	200 × 2	1520× 3	100× 2
2	PWC	6875	500	500	-	6.81	200× 2	1520× 3	100× 2
3	PWU	6875	-	-	1000	6.53	200 × 2	1520× 3	100× 2
4	PWUC	6875	500	500	1000	7.29	1000× 2	1520× 3	500× 2

Table S1. Details of the composition of different solvents and co-solvents and simulation length.
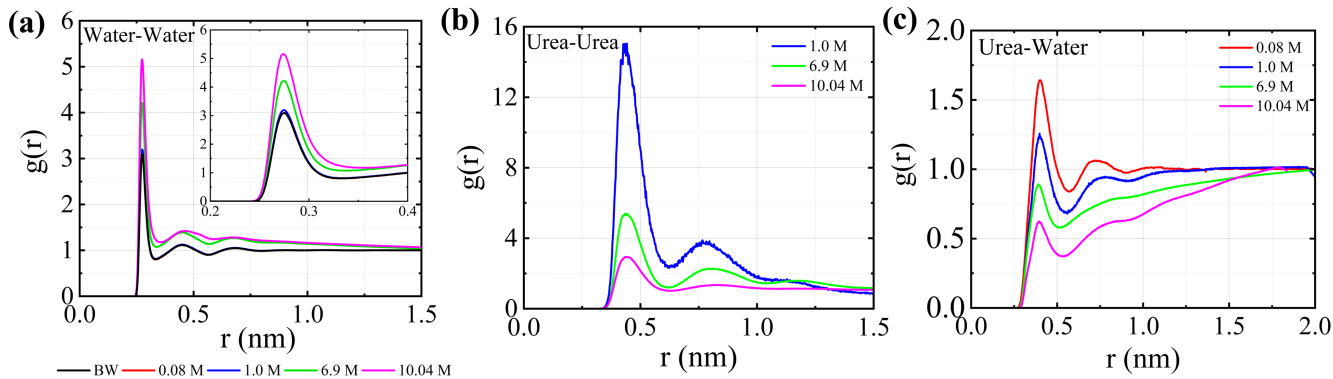
VALIDATION OF OPLS-AA FORCE FIELD FOR UREA

Fig. S2. (a) Water-water, (b) urea-urea, and (c) urea-water radial distribution functions.

Sr. No.	Concentration (M)	Simulated Densities	Earlier Simulation Densities [1]	Experimental Densities [2]	Experimental Densities [3]
1	0.08	998.84	971.2	999.5	998.2
2	1.0	1016.62	989.7	1013.6	1014
3	6.9	1117.09	1096.1	1103.6	1103
4	10.04	1162.65	1156.7	1157.7	1147

Table S2. Comparison of the simulated densities of the investigated aqueous urea solutions of concentrations 0.08 M, 1.0 M, 6.9 M, 10.04 M respectively along with the earlier simulated and experimental densities (at 298 K). All the densities are expressed in Kg/m^3.

We use the OPLS-AA force field to define interaction parameters for urea. To probe the compatibility of the OPLS-AA force field for urea, we study the solvation properties of the urea and water by computing their pair correlation functions. For this purpose, we prepare four different aqueous solutions of urea as 0.08 M, 1 M, 6.9 M, and 10.04 M in accordance with the experimental concentrations to compare the outcomes with the reported experimental observations. The OPLS-AA model for urea reproduces the experimental density for the urea-water system better as shown in Table S2.

Urea Models	Water-Water	Urea-urea	Urea-Water
Our work (OPLS-AA+SPC/E water model)	0.27	0.44	0.40
OPLS-AA (OPLS-AA+TIP4P water model) [4, 5]	0.28	0.45	0.40
KBFF [6, 7]	0.27	0.45	0.39
AMBER [8]	0.27	-	-
Tsai [9]	0.28	0.5	-
TGL-SC, TGL-QC, DKJ [10]	0.27	0.45	0.4
Experiment [11]	0.27	-	-

Table S3. Peak positions of water-water, urea-urea, and urea-water pair correlation functions for investigated solutions along with the other urea models and experimental studies. Units of peak positions are in nm.

Next, we compute pair correlation functions between water-water, urea-urea, and urea-water to better describe urea's

solvation properties and compare them with previously reported simulation and experimental results. A careful observation of water-water g(r) (Fig. S2a) reveals that the peak height increases with increasing urea concentration. Also, the peaks maintain their positions and are almost invariant from pure water to the most concentrated solution of urea. This suggests that urea does not alter the structure of water and this observation is also in agreement with earlier studies using different urea models. A combination of the TIP4P water model along with the OPLS-AA force field parameters including planar and non-planar models for urea based on Monte Carlo simulations accounted for the structuring of water on increasing the concentration of the urea from 5 M to 8 M [4]. The increment in the first peak height for water-water g(r) on increasing urea concentration is also observed for the KBFF model of urea [6]. In another study, Grubmuller and co-workers used OPLS-AA-derived parameters for urea and reported strengthening of water structure in terms of relative population of water in the solvation shells [5]. Other studies employed KBFF and AMBER force field for urea in combination with the TIP4P water model and described urea as a structure maker for the water by computing the distribution of neighboring water from the reference water [8]. The simple charged and quantum charged model representing urea was also adopted by Tsai *et al.*, in conjunction with the iso-steric analogs of urea, showed that even at the highest concentration, urea does not seem to affect the water-water distribution much in comparison to pure water, indicating that urea disperses well in solution [9]. Apart from the simulation data, the role of urea as a structure maker for water is evidenced by experimental techniques such as neutron diffraction [11].

As can be seen from the urea-urea g(r) (Fig. S2b), a peak appears at ∼0.44 nm, and peak height gradually decreases as we increase the concentration of urea from 0.08 M to 10.04 M shows that the average distance between urea molecules around a reference urea molecule is about ∼0.44 nm and does not change with concentration. This similar peak position and the peak height are observed for other studies using the OPLS-AA model of urea [4] and several other models such as KBFF [7], TGL-SC, TGL-QC, DKJ [10]. Moreover, urea-water g(r) shows a similar trend as that of urea-urea provided peak position is at ∼0.40 nm suggesting that the average distance between the center-of-mass of urea and water is ∼0.4 nm (Fig. S2c). This distance is in good agreement with the other urea models [4, 7, 10]. Our results are in good agreement with the previously reported urea models and experimental observations. OPLS-AA reproduces a similar property for urea as that of other models.
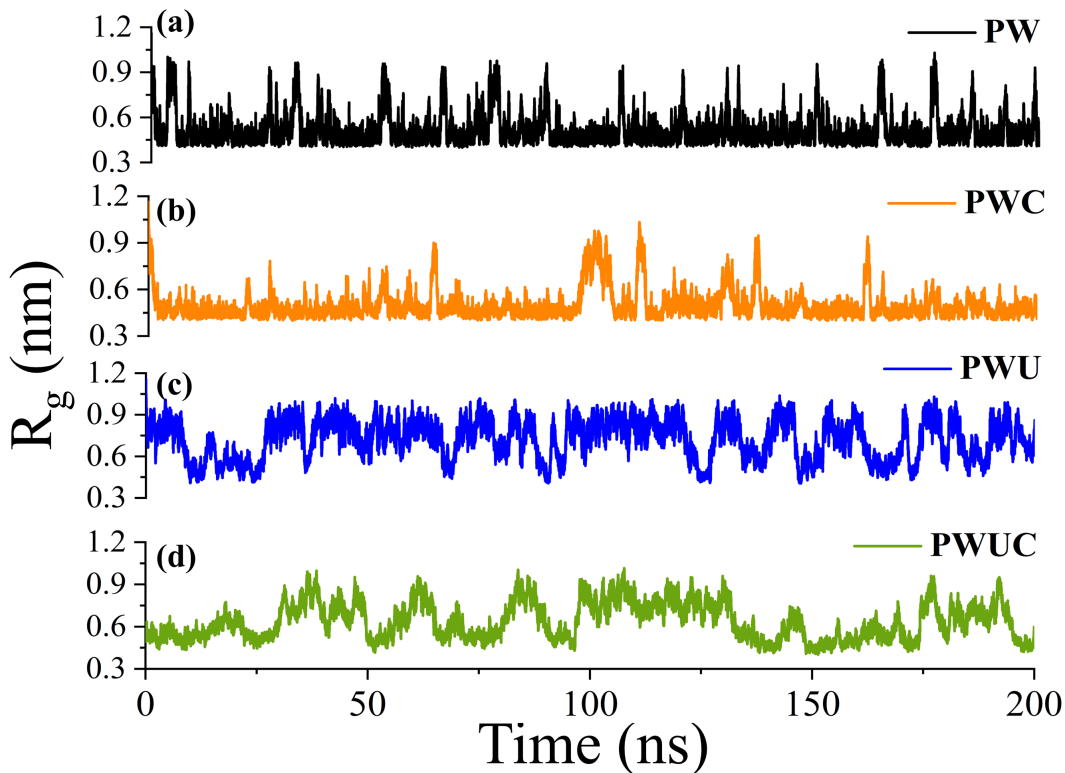

Fig. S3. Time profile of radius of gyration of hydrophobic polymer in (a) PW, (b) PWC, (c) PWU, and (d) PWUC obtained from unbiased simulation. Here, starting configuration of polymer is taken to be extended.

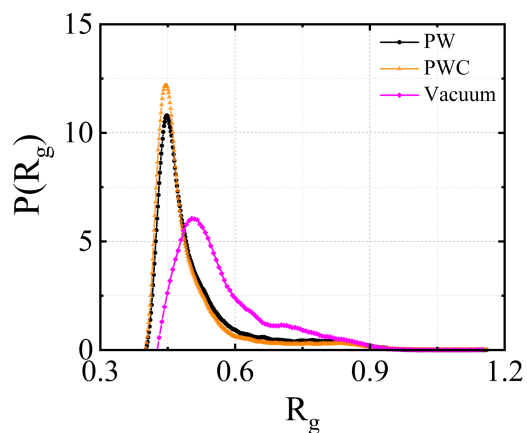**SIMULATION OF A HYDROPHOBIC POLYMER IN VACUUM**

Fig. S4. Probability distribution of radius of gyration, $P(R_g)$ of hydrophobic polymer in vacuum. For comaprison purpose, $P(R_g)$ of hydrophobic polymer in PW and PWC systems are also shown.
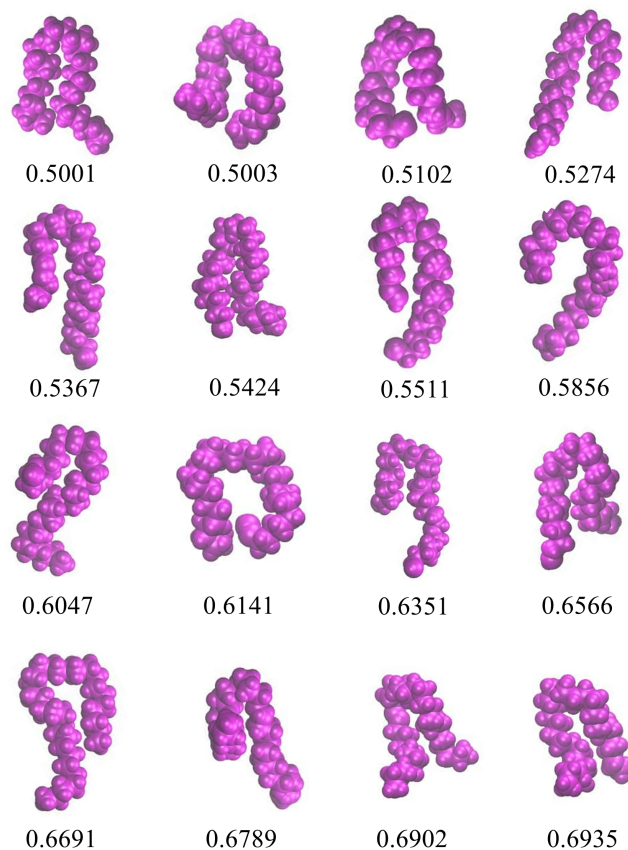
ENSEMBLE ANALYSIS FOR CHOICE OF R_g CUTOFF FOR HAIRPIN STATE

Fig. S5. Random conformations used in ensemble analysis for validating the R_g based cutoff for hairpin states. Values of R_g are in nm.

To verify the choice of cutoff based on R_g values for hairpin states, we extract 50 different intermediate hairpin-like conformations and compute their R_g, which further verifies that R_g values of this conformations lie in the range $0.5 < R_g \leq 0.7$ nm (the cutoff range we used for hairpin state) in most of the cases. Some of the random conformations from this ensemble which correspond to R_g in the range $0.5 < R_g \leq 0.7$ nm shown in Fig. S5. This implies that our choice of Rg-based cutoff is a good measure to differentiate the three different states as supported by the ensemble analysis described here. Moreover, R_g based cutoff to distinguish polymer conformations has been used in earlier studies as well. Our choice of R_g cutoff values is in agreement with the cutoff values reported in the previous works [12, 13, 15]. Hence, we choose this description to categorize the polymer conformations.
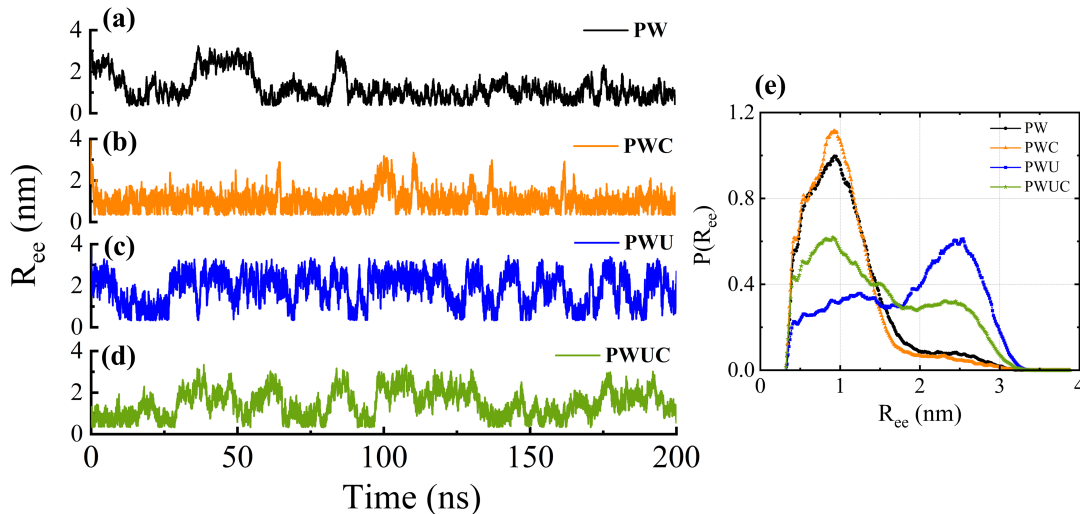

Fig. S6. Time profile of end-to-end distance of hydrophobic polymer in (a) PW, (b) PWC, (c) PWU, and (d) PWUC obtained from unbiased simulations, (e) distribution of end-to-end distance for the polymer in aqueous solution of different osmolytes. Here, starting configuration of polymer is taken to be extended.
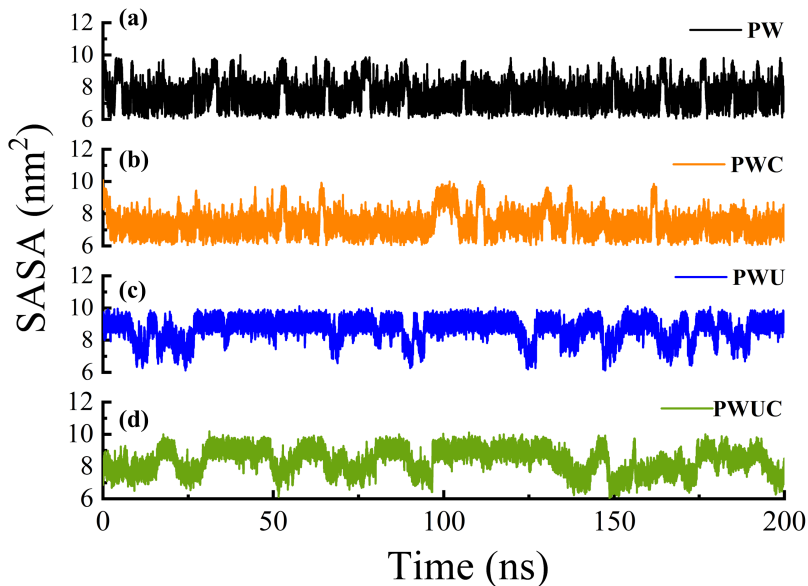

Fig. S7. Time profile of solvent accessible surface area (SASA) of hydrophobic polymer in (a) PW, (b) PWC, (c) PWU, and (d) PWUC obtained from unbiased simulation. Here, starting configuration of polymer is taken to be extended.
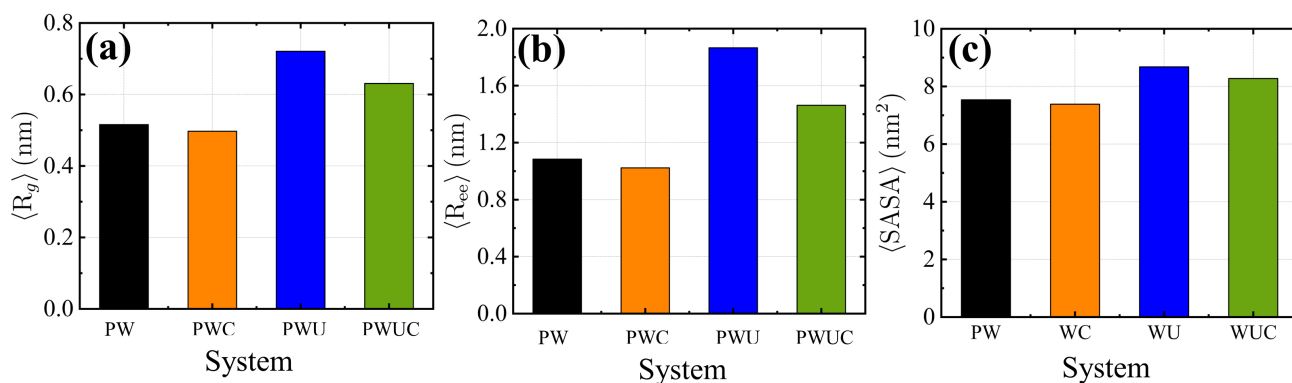
Fig. S8. Average values of (a) radius of gyration, (b) end-to-end distance, and (c) solvent accessible surface area of hydrophobic polymer in different aqueous solutions of osmolyte. Here, starting configuration of polymer is taken to be extended.
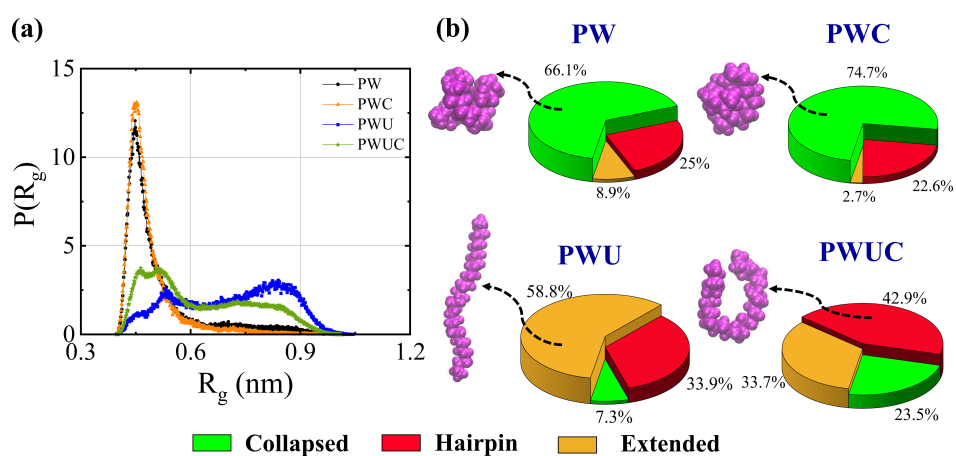

Fig. S9. (a) Probability distribution of radius of gyration, $P(R_g)$ of hydropobic polymer. (b) Percentage of collapsed, hairpin, and extended states for all systems considered. Here, starting configuration of polymer is taken to be collapsed.
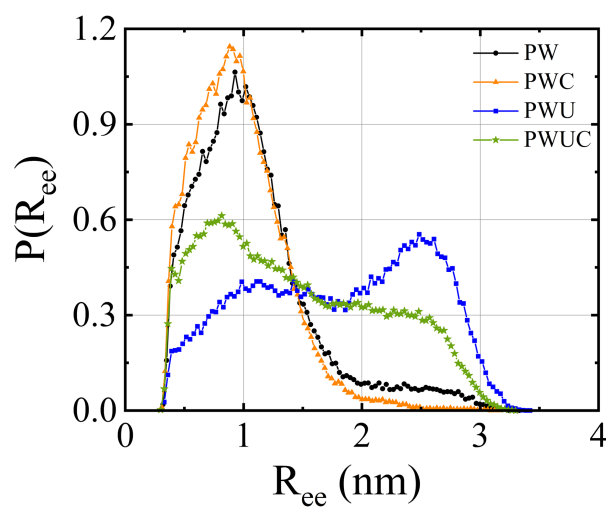

Fig. S10. Distribution of end-to-end distance for polymer in aqueous solution of different osmolytes. Here, starting configuration of polymer is taken to be collapsed.
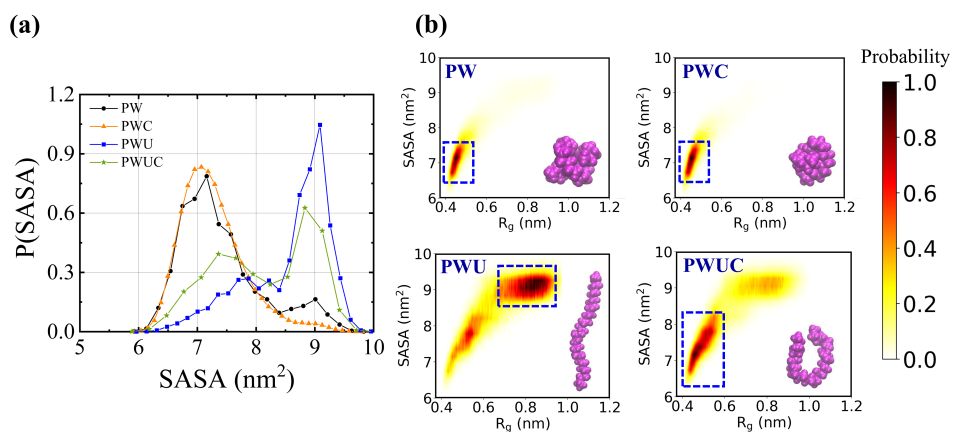
(a)

(b)

Fig. S11. (a) Probability distribution of solvent accessible surface area, P(SASA) of hydropobic polymer, (b) 2D probability distribution of SASA and R_g for all the systems studied. Representative polymer conformations correspond to the highly populated region (highlighted in blue dashed rectangle) are also shown. Here, starting configuration of polymer is taken to be collapsed.
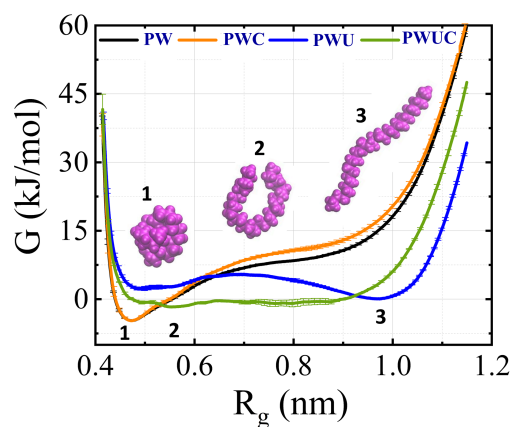

Fig. S12. Free energy (G) of the polymer as a function of R_g for different systems at 320 K temperature. The error bars corresponding to standard deviation are also plotted. Representative polymer conformations corresponding to the three basins are also shown.
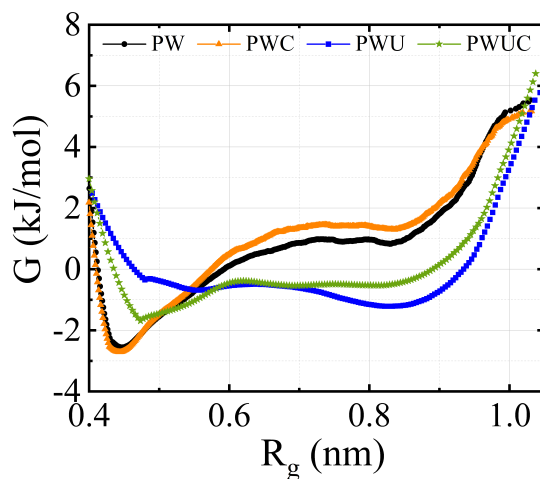

Fig. S13. Free energy (G) of the polymer as a function of R_g for different systems at 300 K temperature obtained from the distribution of R_g (Fig. 2a) from the unbiased simulations.
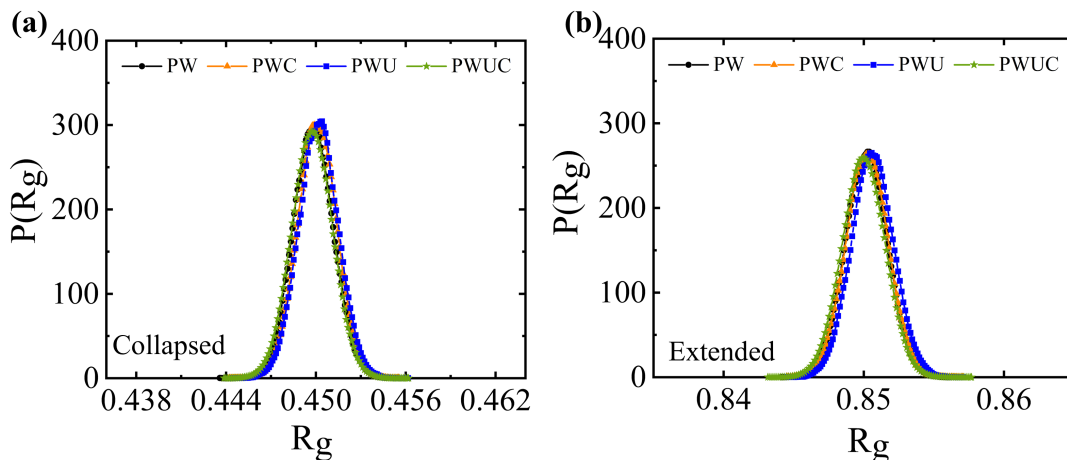
FROZEN STATE SIMULATIONS

Fig. S14. Probability distribution of radius of gyration, P(R$_g$) of hydropobic polymer in frozen (a) collapsed state, (b) extended state.
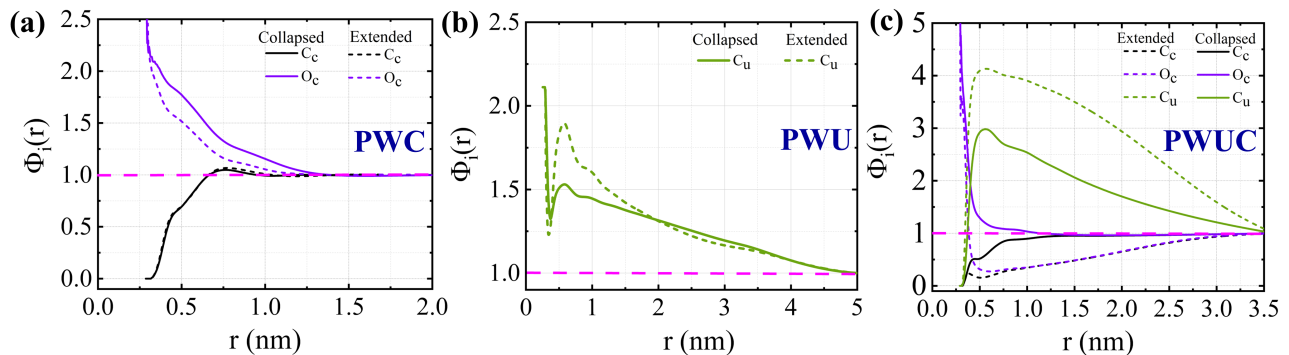
RELATIVE NUMBER FRACTION OF COSOLVENTS

Fig. S15. Relative number fraction $\phi_i(r)$ of (a) hydrophilic part of choline (O$_c$) and hydrophobic part of choline (C$_c$) for PWC system, (b) C$_u$ of urea for PWU system, and (c) hydrophilic part of choline (O$_c$) and hydrophobic part of choline C$_c$, C$_u$ of urea for PWUC system near collapsed and extended states of the polymer as a function of distance (r) from the polymer.

To quantify the relative distribution of solvent and cosolvent around polymer, we compute the relative number fraction $\phi_i(r)$, defined as,

$$\phi_i(r) = \frac{N_i(r)/\sum_i N_i(r)}{N_i(r_{\text{Bulk}})/\sum_i N_i(r_{\text{Bulk}})} \tag{1}$$

where, $N_i(r)$ represents the coordination number of either water, choline, or urea around polymer at distance r, $N_i(r_{\text{Bulk}})$ signifies the coordination number of either water, choline or urea in bulk. Here, 'i' designates the constituent i.e., water, urea, or choline. $\phi_i(r) > 1$ implies an accumulation of the component around polymer and $\phi_i(r) < 1$ implies exclusion. This relative number fraction is doubly normalized with respect to the bulk density and total number of constituents in the system. Hence, it provides a better measure of the relative accumulation or exclusion of constituents from polymer solvation shells.

A careful investigation of Fig. S15a, reveals that in the vicinity of the polymer, $\phi_i(r)$ values of polymer-O_c are greater than 1 whereas, for polymer-C_c, it is less than 1 near both collapsed and extended state of the polymer. This signifies the preferential accumulation and exclusion of hydrophilic and hydrophobic parts of the choline, respectively from the vicinity of the polymer in the PWC system. Comparing $\phi_i(r)$ values of polymer-O_c near collapsed and extended state, it is higher near the collapsed state as compared to the extended state suggesting the accumulation of the hydrophilic part of choline near collapsed state as compared to the extended state. This observation further supports the insights obtained from the preferential binding coefficient of the hydrophilic and hydrophobic part in Fig. 10b. This is responsible for the preference for the collapsed state in the presence of choline i.e., the PWC system. $\phi_i(r)$ values of polymer-C_c appears to be increasing near ~ 0.7 nm which is also reflected in g(r) of polymer-C_c (Fig. 7c).

For PWU system, $\phi_i(r)$ values of polymer-C_u are greater than 1 near both collapsed and extended state (Fig. S15b) indicating the tendency of urea for interacting with the polymer relative to water. However, $\phi_i(r)$ values of polymer-C_u are slightly more near the extended state as compared to the collapsed state because of the stronger interaction of urea near the extended state. These observations are in line with the stronger preferential interaction of urea near the extended state as shown in Fig. 10c. This stronger interaction is responsible for maintaining the extended state as the preferred state in the PWU system.

On the other side, in the PWUC system, $\phi_i(r)$ values of polymer-O_c are greater than 1 near collapsed state but less than 1 near the extended state in the polymer vicinity, however $\phi_i(r)$ values for polymer-C_c are less than 1 near both states. $\phi_i(r)$ for polymer-C_u are greater than 1 near both collapsed and extended state with values near the extended state being larger than the collapsed state (Fig. S15c). This portrays that the hydrophilic part accumulates near the collapsed state while the hydrophobic part is excluded and urea accumulates more near the extended state. This observation of competing interaction goes parallel with the preferential binding coefficient of choline and urea as shown in Fig. 10e. This competing interaction gives rise to the stabilization of the intermediate hairpin state in the presence of both urea and choline.
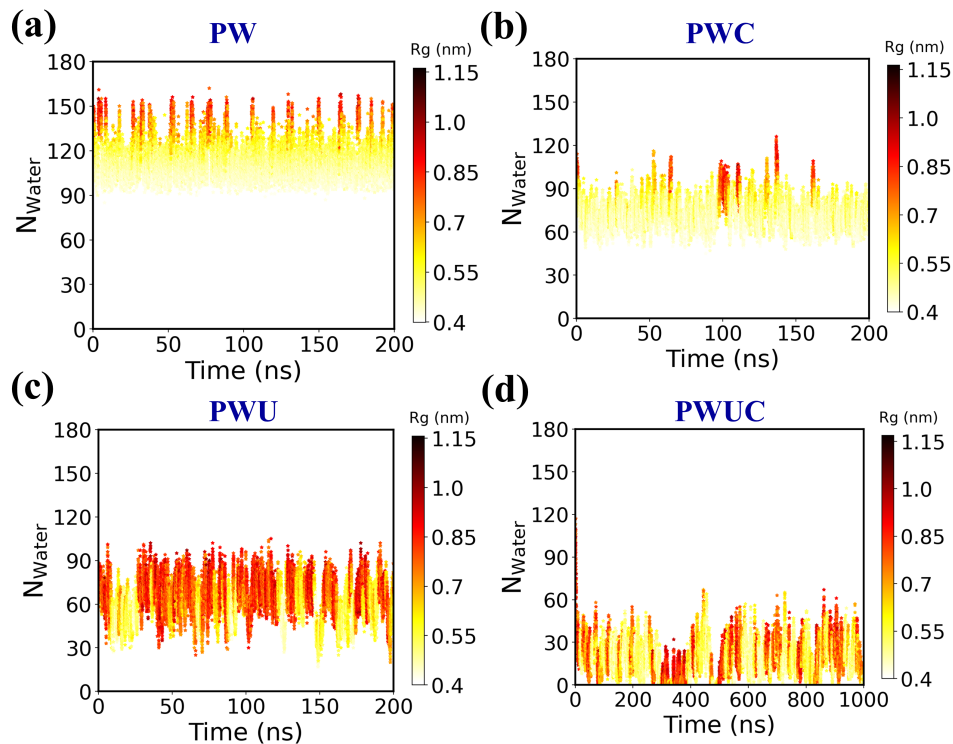

Fig. S16. Number of water molecules (N_{Water}) for different conformations of polymer as function of time for (a) PW, (b) PWC, (c) PWU, and (d) PWUC. Here, starting configuration of polymer is taken to be extended.
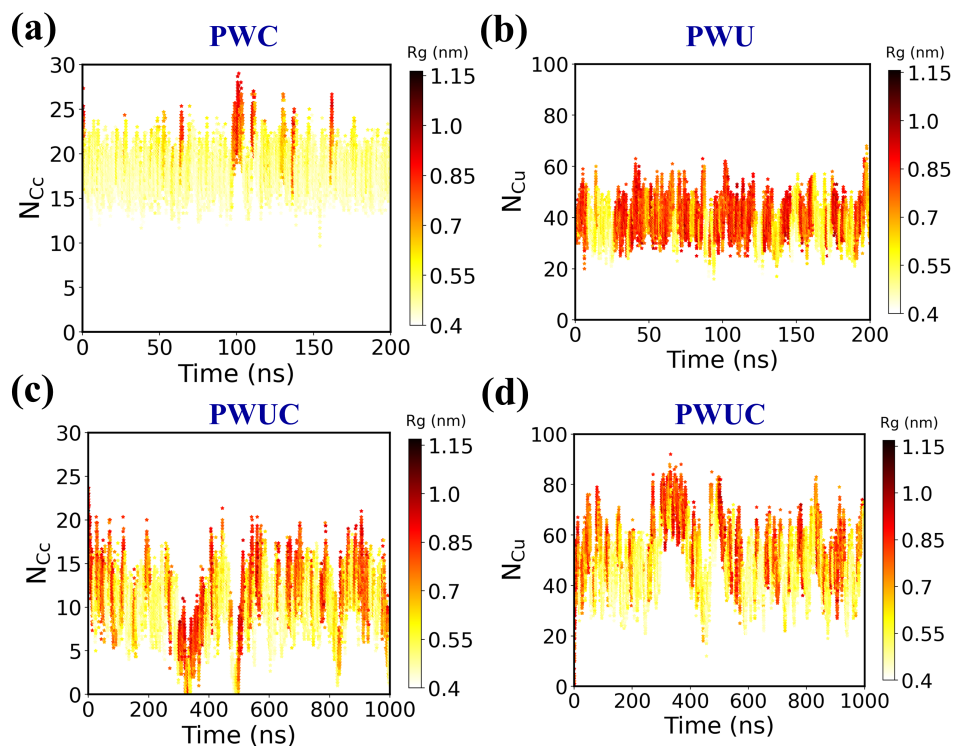
Fig. S17. Number of (a) C_c atoms (N_{Cc}) of choline for PWC, (b) C_u atoms (N_{Cu}) of urea for PWU, (c) C_c atoms (N_{Cc}) of choline for PWUC, and (d) C_u atoms (N_{Cu}) of urea for PWUC for different conformations of polymer as function of time. Here, starting configuration of polymer is taken to be extended.
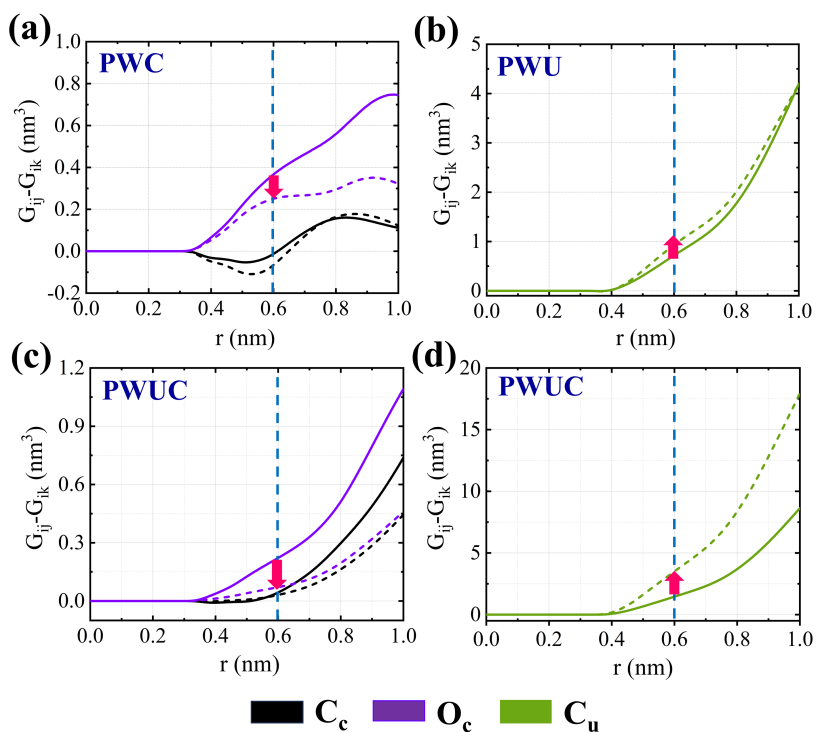

Fig. S18. Preferential Kirkwood-Buff integrals [$G_{ij}(r)$-$G_{ik}(r)$] of (a) C_c and O_c of choline in PWC, (b) C_u of urea in PWU, (c) C_c and O_c of choline, and (d) C_u of urea in PWUC as a function of distance (r) from polymer COM. Here, i stands for polymer and j and k stand for the cosolvent and solvent, respectively. Direction of the arrow denotes the relative sign of [$G_{ij}(r)$-$G_{ik}(r)$]. Here, starting configuration of polymer is taken to be extended.

* rajarshi@chem.iitb.ac.in

[1] L. J. Smith, H. J. Berendsen and W. F. van Gunsteren, *J. Phys. Chem. B*, 2004, **108**, 1065–1071.
[2] D. R. Lide, *Handbook of Chemistry and Physics, 81st ed*, B. Raton, CRC Press, 2000.
[3] K. Kawahara and C. Tanford, *J. Biol. Chem.*, 1966, **241**, 3228–3232.
[4] C. A. Bertran, J. J. Cirino and L. C. Freitas, *J. Braz. Chem. Soc.*, 2002, **13**, 238–244.
[5] M. C. Stumpe and H. Grubmüller, *J. Phys. Chem. B*, 2007, **111**, 6220–6228.
[6] R. D. Mountain and D. Thirumalai, *J. Phys. Chem. B*, 2004, **108**, 6826–6831.
[7] S. Weerasinghe and P. E. Smith, *J. Phys. Chem. B*, 2003, **107**, 3891–3898.
[8] D. Bandyopadhyay, S. Mohan, S. K. Ghosh and N. Choudhury, *J. Phys. Chem. B*, 2014, **118**, 11757–11768.
[9] J. Tsai, M. Gerstein and M. Levitt, *J. Chem. Phys.*, 1996, **104**, 9417–9430.
[10] F. Sokolić, A. Idrissi and A. Perera, *J. Mol. Liq.*, 2002, **101**, 81–87.
[11] J. Finney, A. Soper and J. Turner, *Phys. B: Condens. Matter*, 1989, **156**, 151–153.
[12] D. Nayar and N. F. van der Vegt, *J. Phys. Chem. B*, 2018, **122**, 3587–3595.
[13] M. Mukherjee and J. Mondal, *J. Phys. Chem. B*, 2019, **123**, 8697–8703.
[14] M. Mukherjee and J. Mondal, *J. Phys. Chem. B*, 2019, **123**, 4636–4644.
[15] J. Mondal, G. Stirnemann and B. Berne, *J. Phys. Chem. B*, 2013, **117**, 8723–8732.